CrossMark

ORIGINAL PAPER

Optimal fractional order adaptive controllers for AVR applications

Marco E. Ortiz-Quisbert[1,2] · Manuel A. Duarte-Mermoud[1,2] · Freddy Milla[1,2] ·
Rafael Castro-Linares[3] · Gastón Lefranc[4]

Abstract This work presents strategies for fractional order model reference adaptive control (FOMRAC) and fractional order proportional–integral–derivative control (FOPID) applied to an automatic voltage regulator (AVR). The paper focuses on tuning the gains and orders of the FOPID controller and the gains and orders adaptive laws of the FOMRAC controller, with the goal of minimizing non-linear and high dimensionality objective functions, using sequential quadratic programming (SQP), particle swarm optimization (PSO), and genetic algorithms (GA). Two models used for AVR have been studied and reported in the literature and are the bases of the three case studies reported in this paper. To analyze the advantages and disadvantages of the proposed MRAC, comparisons are made with the previous results, i.e. with the results obtained by a PID controller and an MRAC controller optimized by GA. We demonstrate through some performance criteria that fractional order controllers optimized by the PSO algorithm improve the behavior of the controlled system, specifically the robustness with respect to model uncertainties, and improvements with respect to the speed convergence of the signals.

Keywords Fractional order adaptive control · Model reference adaptive control · Automatic voltage regulator · Particle swarm optimization · Genetic algorithms · Sequential quadratic programming

✉ Manuel A. Duarte-Mermoud
mduartem@ing.uchile.cl

Marco E. Ortiz-Quisbert
marco.ortiz@ing.uchile.cl

Freddy Milla
fmilla@ing.uchile.cl

Rafael Castro-Linares
rcastro@cinvestav.mx

Gastón Lefranc
glefranc@ucv.cl

1   Electrical Engineering Department, University of Chile, Av.
    Tupper 2007, Santiago, Chile

2   Advanced Mining Technology Center (AMTC), University of
    Chile, Av. Tupper 2007, Santiago, Chile

3   Department of Electrical Engineering, CINVESTAV-IPN, Av.
    IPN 2508, Mexico City, D.F., Mexico

4   School of Electrical Engineering, Pontificia Universidad
    Católica de Valparaíso, Av. Brasil 2147, Valparaiso, Chile

1 Introduction

Power systems not only require devices that maintain and ensure their stability, but also require increasingly quick response times. The most important feature of a control scheme is that, it tunes its parameters in response to the uncertainties caused by changes in the operating conditions of the system. Model reference adaptive control (MRAC) is one of such techniques, which has the aim of finding a suitable control signal so that the output of the controlled system follows the output of the reference model, while at the same time, the stability of the closed loop system is preserved. Optimization algorithms, such as SQP, heuristic methods like GA, and algorithms based on groups like PSO, which optimize parameters minimizing an objective function (OF) considering several variables, are used to meet quick response times. The application of fractional calculus, which generalizes the classical differential calculus of integer order $\frac{dx(t)}{dt}$ to the calculus of fractional order $\frac{d^\alpha x(t)}{dt^\alpha}$ is included in our study. This generalization is reflected by the extent of the search range which is used by algorithms to improve the minimization of cost functions.

Gaing [11], showed improvements on tuning PID controller parameters by minimizing an objective function optimized by PSO. Later, in [8], the authors used the same simplified linear model (SLM) of the generator that was used in [11], and introduced improvements in the optimization process based on a modification of PSO algorithm. Tang et al. [32], introduced chaotic characteristics (chaotic ant swarm) in the tuning process of the PID controller parameters, showing significant improvements over all previous methods, including GA. These authors considered variations of $\Delta V_r(t) = 1$ (pu) for comparing optimization strategies in terms of the minimum of a given cost function, where $\Delta V_r(t)$ denotes the variation of the reference voltage with respect to a nominal value. In [21], the previous SLM is used, but the authors use $\Delta V_r(t) = 0.01$ (pu), minimizing a cost function using the PSO method. Later, in [7] the same features as those in [21] are applied; however, another change to PSO was proposed, which showed improvements in minimizing the cost function.

Another control scheme introduced in the context of AVR systems with SLM, is fuzzy logic [30]. And, there have been proposals made of using the linear model (LM) of the generator proposed by Kundur [16], which also considers the mechanical characteristics of the synchronous machine. These features are used in optimization problems in [37], where the parameters of the PID controller are selected by the PSO algorithm. The latter introduces concepts of fractional calculus. In [1], the FOMRAC is proposed. It is considered as an optimization problem and solved by GA, under the same operating conditions that were reported in [37] and showed better results, in terms of robustness and the minimization of the cost function, than those reported in [37].

In our work, the FOMRAC technique is regarded as an optimization problem, in which gains and orders of adaptive laws defined by fractional-order differential equations are adjusted. These are based on objective functions subject to constraints provided by the LM and the SLM of the generator. They are detailed in the following paragraphs. This FOMRAC shows improvements in response characteristics and in robustness with respect to model uncertainties, reducing the value of the cost function up to 64% and yielding improvements up to 69% in terms of t_s compared with those found in the literature. Three case studies are proposed and will be analyzed in this paper. To our knowledge, these three cases have not been previously reported and constitute the main aim of the paper together with the comparative analysis with numerous cases already studied in the technical literature.

The paper is organized as follows: Sect. 2 introduces general concepts of direct FOMRAC. It also introduces the concepts of optimization algorithms and models used in each case study. Section 3 establishes the conditions, the characteristics of the controller, and the objective functions.

Section 4 presents experimental results, comparing the different control techniques and optimization strategies with results previously reported in the literature. Finally, Sect. 5 presents the conclusions.

2 General concepts

The main theoretical principles used in this work are presented in this section.

2.1 Fractional calculus

Fractional calculus is a generalization of the traditional calculus and is related to differential operators of type D_t^α, where α is a real or complex number. According to Kilbas [15], the Riemann–Liouville (RL) fractional order integral is defined as

$$^R D_0^\alpha f(t) = \frac{1}{\Gamma(n-\alpha)} \left(\frac{\mathrm{d}}{\mathrm{d}\tau}\right)^n \int_0^t \frac{f(\tau)}{(t-\tau)^{\alpha-n+1}} \mathrm{d}\tau \qquad (1)$$

with $n = [\Re(\alpha)] + 1$; $t > \alpha$, where $[\Re(\alpha)]$ is the integer part of $\Re(\alpha)$.

In most engineering applications, for $\alpha > 0$, the Caputo derivative definition found in (2) is used since it incorporates initial conditions for $f(\cdot)$ i.e., initial conditions that are physically interpretable in the traditional way.

$$^C D_0^\alpha f(t) = \frac{1}{\Gamma(n-\alpha)} \int_0^t \frac{f^{(n)}(\tau)}{(t-\tau)^{\alpha-n+1}} \mathrm{d}\tau \qquad (2)$$

with $n - 1 < \alpha < n$ and $n \in \mathbb{Z}^+$.

Oustaloup's method [25] allows to make approximations of non-integer derivatives. It is one of the available frequency-domain methods that uses a recursive distribution of N poles and N zeros of the form

$$s^\alpha \approx k \prod_{n=1}^{N} \frac{1 + (s/\omega_{z,n})}{1 + (s/\omega_{p,n})} \qquad (3)$$

with $\alpha > 0$. Moreover, the frequencies of the poles and zeros ($\omega_{z,n}$ and $\omega_{p,n}$) are given by [37]. Zeros and poles are placed inside a frequency interval $[\omega_l; \omega_h]$, and the gain k is adjusted so that the gain on both sides of (3) is 1 rad/s. The number of poles and zeros N is chosen in advance, and the desired performance of the approximation strongly depends on: low values cause simpler approximations, but may cause ripples in both gain and phase behaviors. Such ripples can be removed functionally by increasing the N, but the approximation will become heavier computationally. This approximation is available in the Ninteger toolbox for

Matlab [34], and is the one used in the work reported in this paper.

2.2 Fractional order model reference adaptive control

Some pioneering works in the context of the FOMRAC are due to Vinagre et al. [35] and Ladaci et al. [17,18]. For the classic direct MRAC, the controller parameters are adjusted using integer order differential equations (adaptive laws). However, this paper focuses on the direct FOMRAC, in which the parameters are adjusted adaptively using fractional-order differential equations (fractional adaptive law) keeping the same structure of direct MRAC [23]. Thus, this section begins by giving a brief introduction to classical MRAC. For real-life applications, some uncertainties are the result of the parameters being unknown. On the other hand, there are existing systems that can be only partially modeled due to external disturbances. In these cases, conventional control theory has not achieved satisfactory performance, while in the direct MRAC, the parameters of the controller are directly adjusted; that is to say, no identification of the plant parameters is attempted [23]. Given a known reference model $G_m(s)$, a reference signal $r(t)$ is applied to obtain the measurable output $y_m(t)$. This output is compared with the AVR output voltage $y_p(t)$ to compute the control error defined as $e_1(t) = y_p(t) - y_m(t)$. In this paper, we will use $y_p(t) = \Delta V_T(t)$, $y_m(t) = \Delta V_M(t)$ and $u(t) = \Delta u(t)$ for Table 1 (see Fig. 1). Since the relative degree of the system to be analyzed here is $n* \geq 2$, the control scheme is shown in Fig. 1.

The details of the scheme of Fig. 1 can be found in [1]. However, when $n^* \geq 2$, there are some concepts that should be noted; an augmented error $\epsilon(t)$ is synthesized that permits stable adaptive laws to be implemented, and the auxiliary error signal $e_2(t)$ is generated. The most important details of this controller are shown in Table 1, in which n is the system order, so, $n - p = n^*$ and $q = n^*$, with q the model reference order. The size of the matrices (Λ, l), and the number of parameters to optimize will be defined in Sect. 3.

2.3 Optimization algorithms

Basic concepts associated with optimization algorithms used in this work are presented in this section.

2.3.1 Particle swarm optimization

PSO is a heuristic global optimization technique which belongs to the category of evolutionary search algorithms [14]. It solves optimization problems based on the behaviour of existing virtual social groups in nature (flocks of birds, swarms, etc.) as reported by Ordóñez [24]. Furthermore, the method has shown improvements in minimizing cost func-

Table 1 General fractional order MRAC

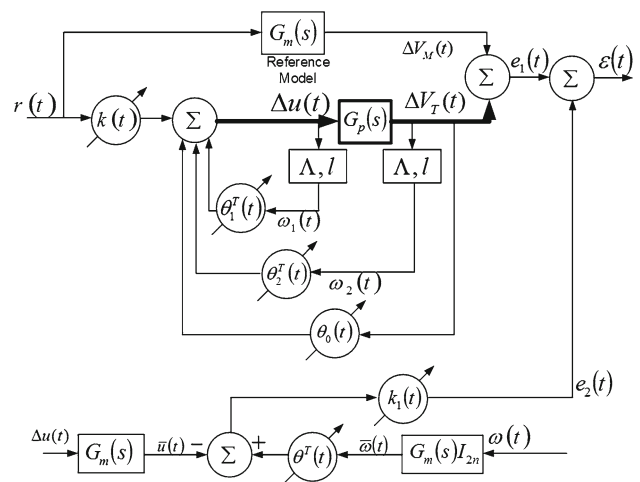|	
Plant	$G_p = \frac{b_p s^p + b_{p-1} s^{p-1} + \cdots + b_1 s + b_0}{a_n s^n + a_{n-1} s^{n-1} + \cdots + a_1 s + a_0}$
Reference model	$G_m = \frac{k_m}{m_q s^q + m_{q-1} s^{q-1} + \cdots + m_1 s + m_0}$
Control law	$u(t) = \theta(t)^T \omega(t)$
	$\theta(t)^T = [k(t)\ \theta_1^T(t)\ \theta_0(t)\ \theta_2^T(t)]$
	$\omega(t) = [r(t)\ \omega_1^T(t)\ y_p(t)\ \omega_2^T(t)]$
Auxiliary signals	$\dot{\omega}_1(t) = \Lambda \omega_1(t) + lu(t)$
	$\dot{\omega}_2(t) = \Lambda \omega_2(t) + ly_p(t))$
	$\lambda = \begin{bmatrix} \Lambda_1 & 0 & 0 & 0 \\ 0 & \ddots & 0 & 0 \\ 0 & 0 & \ddots & 0 \\ 0 & 0 & 0 & \lambda_{n-1} \end{bmatrix}$
	$l = [\ell_1\ \ldots\ \ldots\ \ell_{n-1}]^T$
Output error	$e_1(t) = y_p(t) - y_m(t)$
Auxiliary error	$e_2(t) = \theta^T(t)\bar{\omega}(t) - \bar{u}(t)$
Augmented error	$\epsilon(t) = e_1(t) + k_1(t)e_2(t)$
Other signals	$\bar{u}(t) = G_m(s)I_{2n}u(t)$
	$\bar{\omega}(t) = G_m(s)I_{2n}\omega(t)$
Adaptive laws	$D^\alpha \theta(t) = -\gamma \frac{\epsilon(t)\bar{\omega}(t)}{1 + \bar{\omega}(t)\bar{\omega}^T(t)}$
	$D^\alpha k_1(t) = -\gamma \frac{\epsilon(t)e_2(t)}{1 + \bar{\omega}(t)\bar{\omega}^T(t)}$

Fig. 1 Block diagram for the implementation of the FOMRAC for the AVR [1]

tions, particularly when they have non-linear characteristics, multiple optimal values, and high dimensionality [37]. The individuals defined as potential solutions are particles that evolve iteratively according to different strategies to find the best possible global solution from a set of equations that update the velocity (4) and the position (5) of each particle in the search space [11].

$$v_{\text{id}}^{(t+1)} = w^{(t)}v_{\text{id}}^{(t)} + c_1 r_1^{(t)}(p_{\text{id}}^{(t)} - x_{\text{id}}^{(t)}) + c_2 r_2^{(t)}(p_g^{(t)} - x_{\text{id}}^{(t)}) \tag{4}$$

$$x_{\text{id}}^{(t+1)} = x_{\text{id}}^{(t)} + v_{\text{id}}^{(t+1)} \tag{5}$$

where w_{iter} represents the inertia factor that is directly related to exploration ($w_{\max}$) and exploitation ($w_{\min}$) of the search space. This decreases as the iterations progress according to Eq. (6) [31].

$$w_{\text{iter}} = w_{\max} - \frac{w_{\max} - w_{\min}}{\text{iter}_{\max}} \cdot \text{iter} \tag{6}$$

where $iter_{\max}$ represents the maximum number of iterations allowed by the search algorithm. c_1 and c_2 correspond to the cognitive and social constants for (4). These constants affect the rate of convergence of each particle. The variables r_1, r_2 with uniform distribution contribute to the stochastic environment, i.e. $r_1, r_2 \sim U[0, 1]$. At the same time, these variables prevent particles from stagnating in a local optimum. For further details of the evolution of the PSO algorithm, see reference [37].

2.3.2 Genetic algorithms

GA is a method used to solve constrained or unconstrained optimization problems. These are based on natural selection processes which, in turn, are the basis of the biological evolution. The GA modifies a population of possible individual solutions iteratively. At each step, the genetic algorithm selects individuals at random from the current population. This population evolves over generations to produce better solutions to the problem. These algorithms can be applied to solve a variety of optimization problems that are not well suited for standard optimization algorithms, including problems in which the objective function is discontinuous, non-differentiable, stochastic, or highly non-linear. GA uses three main types of rules at each step to create the next generation of the population.

- *Selection rules* Select the individuals, called parents, that contribute to the population at the next generation.
- *Crossover rules* Combine two parents to form children for the next generation.
- *Mutation rules* Apply random changes to individual parents to form children.

For more details about the specific steps taken by the algorithm, see reference [20].

2.3.3 Sequential quadratic programming

Recently, considerable progress in the development of general-purpose optimization techniques for SQP has been reported in the literature [4,10]. These methods consider non-linear optimization, which is efficient and can be applied to large problems including linear and non-linear constraints. These methods require very few evaluations of the objective function and converge to a solution depending on the initial conditions of the problem. In general, the problem of optimizing a non-linear function subject to constraints can be written as:

$$\begin{aligned} & \underset{x \in R^n}{\text{minimize}} \ \text{OF}(x) \\ & \text{subject to } b_l \leq \left\{ \begin{array}{c} Ax \\ c(x) \end{array} \right\} \leq b_u \end{aligned} \tag{7}$$

where c is a vector defining the non-linear constraints, A is a constant that defines the parameters of the linear constraints, and b_l and b_u are vectors defining the upper and lower bounds of each constraint, respectively. $\text{OF}(x)$ is a generic objective function (OF) of certain vector variable x. In this study, two OFs are used and they are defined in Eqs. (12) and (13) denoted as OF_1 and OF_2, respectively. The basic idea of SQP is to solve the objective function from a given approximate solution x^k through the formulation of a quadratic programming sub-problem. Then, it uses this sub-problem to build the best approximation of x^{k+1}. This process is iterated so that the expected solution converges to an optimal solution x^* [5].

According to Boggs [5], the correct choice of the sub-problem reduces SQP to Newton's method, with fast convergence. However, the presence of constraints causes both analyses to be significantly different. Two additional properties of this method are worth mentioning:

- SQP is not a feasible point method. The initial condition or some subsequent point generated by the algorithm will not necessarily be within the feasible solution space. A feasible point is one that satisfies all the constraints associated with the objective functions.
- The success of the SQP method depends on the existence of a fast and accurate algorithm for solving quadratic programs.

According to [19], Matlab uses the "fmincon" function which is configured to use this method.

2.4 Automatic voltage regulators

Generators often work at constant voltage through an AVR system which controls the terminal voltage through the excitation system. It makes the terminal voltage equal to the reference voltage [6]. Among the many events that cause voltage drop, reactive power transmitted through a line has a great impact on the voltage profile. It can also cause large voltage drops, and, therefore, should be avoided. Currently,

there are alternatives to maintaining the generated voltage within a specified range [2]. However, our work focuses on the design of an AVR system, which is the most effective way to control the voltage in most power systems. The AVR system is composed of subsystems, which are the amplifier, exciter, generator, and sensor.

2.4.1 Generator models

Synchronous machines are the main source of power generation systems, and their stability depends mostly on maintaining synchronous operation [36]. Therefore, the understanding of the characteristics and the modeling of the dynamic behavior is of critical importance for the study of the stability of electric power systems. Thus, this paper presents two common dynamic models for the generator.

Model$_1$ Figure 2 shows the block diagram of an LM associated with the generator model that considers whole mechanical and electrical phenomenology. This model considers the amplifier, exciter and sensor block diagrams (same as in Model$_2$), but the transfer function of the generator from ΔV_E to ΔV_T considers the electrical and mechanical parameters and it is of third order (whereas in Model$_2$ is of first order only). $K_1, K_2, \ldots, K_6$ are electrical and mechanical machine parameters describing the generator [16]

This representation is far more general than the Model$_2$ described below and it was taken from [16].

Model$_2$ In this case, the transfer function considers a simplified relationship between the field voltage ΔV_E and generator terminal voltage ΔV_T. This relationship can be expressed in terms of the gain K_G and a time constant τ_G, and is given by Gaing et al.[11], Mukherjee et al. [22] and Tang et al.[32]. Its transfer function is given by

$$G_g(s) = \frac{K_G}{1 + \tau_G s} = \frac{\Delta V_T}{\Delta V_E}, \tag{8}$$

while the block diagram for analyzing this case is presented in Fig. 3, whose values were taken from [7].

2.4.2 Amplifier model

The amplifier model [11] is presented by the gain K_A and a time constant τ_A, whose transfer function is

$$G_a(s) = \frac{K_A}{1 + \tau_A s} = \frac{\Delta V_A}{\Delta u}. \tag{9}$$

2.4.3 Exciter model

The main function of the excitation system is to supply energy in the form of direct voltage and current to the generator field, creating a magnetic field. Its transfer function is given by

$$G_e(s) = \frac{K_E}{1 + \tau_E s} = \frac{\Delta V_E}{\Delta V_A}, \tag{10}$$

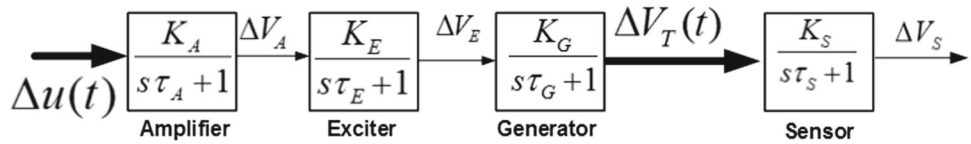while the gain K_E and time constant τ_E will be defined in Sect. 3.2

2.4.4 Measurement model

The voltage measurement block, including a rectifier and filter, is often modeled with a single time constant

$$G_s(s) = \frac{K_S}{1 + \tau_S s} = \frac{\Delta V_S}{\Delta V_T}, \tag{11}$$

while the gain K_S and time constant τ_A will be defined in Sect. 3.2

Fig. 2 Block diagram of the first generator model

$$OF_2 = (w_1 O_s)^2 + w_2 t_s^2 + \frac{w_3}{(\max - \mathrm{d}v)^2} \tag{13}$$

Equation (13) contains to $[\alpha^T \; \gamma^T] \in \Re^{10}$ subject to $0 < \alpha \le 2$ and $0 < \gamma \le 9 \times 10^8$.

According to Panda et al. [28], it should be noted that additional performance criteria are proposed for determining the efficiency of each control technique. These are the integral of the absolute error (IAE), the integral of the time-weighted absolute error (ITAE), the integral of the squared error (ISE), and the integral of the time-weighted squared error (ITSE).

3 AVR design using MRAC and optimization algorithms

This section introduces the values for the AVR parameters, and presents the design procedure of the FOMRAC and optimization algorithms.

3.1 Performance criteria

There are several performance criteria for designing controllers. This paper, however, includes only two objective functions, which have been used by other authors.
OF_1 To achieve system performance according to control specifications, the first performance criterion used in the optimization process is defined according to [1,37] as

$$OF_1 = w_1 O_s + w_2 t_s + w_3 E_{ss}$$
$$+ w_4 \int_0^{t_f} |e_c(t)| \mathrm{d}t + w_5 \int_0^t u^2(t) \mathrm{d}t \tag{12}$$

When a FOMRAC strategy is used, Eq. (12) depends on vector $[\alpha^T \; \gamma^T] \in \Re^{22}$, a vector representing the derivative orders (vector $\alpha \in \Re^{11}$) and the adaptive gains (vector $\gamma \in \Re^{11}$) for the adaptive laws of the controller parameters. (See last row of Table 1). Thus, the optimization procedure for (12) is performed in a 22-dimensional space. To reduce the search space, each component of vectors α and γ is constrained to $0 < \alpha_i \le 2$, $0 < \gamma_j \le 100$, and the final time is $t = 100$. If the IOMRAC strategy is employed, function OF_1 depends on 11 parameters only since the derivative order of the adaptive laws is fixed to 1 and only the adaptive gain can be varied.

This performance criterion includes the overshoot O_s, settling time t_s, steady-state error E_{ss}, integral of absolute error IAE with $e_c(t) = r(t) - \Delta V_T(t)$ as the control error, and $r(t) = \Delta V_r(t)$. The control signal generated by the FOMRAC is $\Delta u(t)$. Several trials were performed for the optimization process, using values for the weighting factors close to the values used in Aguila-Camacho et al. [1]. The smallest value of OF_1 was obtained for $w_1 = w_2 = w_4 = 1$, $w_3 = 1000$ and $w_5 = 7$.
OF_2: Chatterjee et al. [7] defined the objective function as Equation (13) [21,22] which corresponds to minimum overshoot O_s, minimum settling time t_s, and $\max - \mathrm{d}v$ (Maximum point of the voltage signal derivative). The values for the weighting factors are $w_1 = 10000$, $w_2 = 1$ and $w_3 = 0.001$ from [7].

3.2 Design of the MRAC

Two case studies, depending on the model of the generator used, were analyzed as described below.

3.2.1 Case 1

As mentioned in Sect. 2.4, the first model used in this case study corresponds to Model$_1$ shown in Fig. 2 in which the parameters are $K_A = 10$, $\tau_A = 0.1$ (s), $K_E = 1$, $\tau_E = 0.5$ (s), $K_1 = 1.591$, $K_2 = 1.5$, $K_3 = 0.333$, $K_4 = 1.8$, $K_5 = -0.12$, $K_6 = 0.3$, $\tau_3 = 1.91$ (s), $H = 3$, $K_D = 0$, $\omega_0 = 377$ (rad/s), $K_S = 1$, and $\tau_S = 0.06$ (s). These parameters were taken from [1,16].

For fractional adaptive controller design purposes, the plant to be controlled has a sixth-order transfer function. However, since the dynamic of the sensor is very fast, its influence in the transfer function can be ignored. The plant transfer function $G_p(s)$ is then considered as one of the fifth order and with relative degree $n^* = 3$. According to Narendra et al. [23], the reference model $G_{m1}(s)$ has to be chosen with a relative degree greater or equal to the plant relative degree, as is shown in (14) and as used in Aguila-Camacho et al. [1].

Parameters of the auxiliary signal and the reference model (14) for this Case 1 are $p = 2$, $b_2 = 5.994$, $b_1 = 0$, $b_0 = 825.2$, $a_5 = 0.573$, $a_4 = 7.176$, $a_3 = 72.36$, $a_2 = 706.6$, $a_1 = 1302$, $a_0 = 260.8$, $\mathrm{Diag}(\Lambda) = [-1 \; -2 \; -3 \; -4]$, and $l = [-1 \; 1 \; 3 \; 4]^T$. This first application included the optimization of 11 parameters for the case of the IOMRAC (Integer Order MRAC) controller and 22 parameters for the FOMRAC controller.

$$G_{m1} = \frac{1.2}{s^3 + 5.2s^2 + 7s + 1.2} \tag{14}$$

It is interesting to note here that an FO model reference could also be chosen in the scheme, as long as some freedom on this choice is allowed in the controller design, and more importantly, the stability of the resulting overall adaptive system is preserved. This topic is currently being investigated [12].

To compare different control techniques and optimization strategies, MRAC controller parameters are adjusted, considering a unit step $\Delta V_r(t) = 1$ (pu) as input.

3.2.2 Case 2

The model used in this case is shown in Fig. 3. According to Chatterjee et al. [7], the values of the constants are: $K_A = 10$, $K_E = 1$, $K_G = 0.7$, $K_S = 1$, $\tau_A = 0.1$, $\tau_E = 0.4$, $\tau_G = 1$ and $\tau_S = 0.01$. The open loop transfer function of the AVR system is a 4th order model, i.e., that the IOMRAC controller has nine parameters to adjust. As in Case 1, if the dynamic of the sensor can be ignored, then the system is a third-order model. However, the dynamic of the system can be considered as one of the 2nd order, because its step response is similar to the third-order system. Then, the controller will adjust just 5 parameters for the IOMRAC controller and 10 parameters for the FOMRAC controller. Beyond this, selection of the reference model is the responsibility of the control designer, and will be chosen according to the requirements to be met by the control scheme. In this case, given the characteristics of the power generation process, a smooth step response is desired. Also, a small overshoot and settling time, and minimal steady-state error. To satisfy these requirements, the reference model was selected as in (15) and the parameters of the auxiliary signals are $\text{Diag}(\Lambda) = [-20]$, $l = [1]$ from Table 1.

$$G_{m2} = \frac{630}{21s^3 + 159.8s^2 + 524.8s + 630} \quad (15)$$

To compare with previous results, the parameters are adjusted taking as reference voltage $\Delta V_r(t) = 0.01$ (pu). This is used in Chatterjee et al. [7].

3.3 Design of optimization algorithms

In this section, the parameters of the three optimization algorithms used in each proposed study case are defined.

3.3.1 Case 1

Limited by practical requirements, the lower bounds of the controller parameters (α and γ) are $\text{LB}_\gamma = 0.1$ and $\text{LB}_\alpha = 0.01$, respectively. The upper bounds are $\text{UB}_\gamma = 100$ and $\text{UB}_\alpha = 2$, respectively, which belong to the gains and orders of adaptive laws. For the FOMRAC controller, ω_l and ω_h in

(3) are set to 0.001 and 1000(rad/s), respectively, and the order of approximation in (3) is set to $N = 10$. For the PSO algorithm, the parameters used by [7] are defined as follows:

- The initial population cannot be chosen as in the literature, because this work is optimizing triple the number of parameters, and since the number of initial individuals is specific to each problem, 150 particles are defined.
- Inertia weight factor is set as (6), where $w_{\max} = 1.9$ and $w_{\min} = 0.4$.
- Acceleration constants $c_1 = c_2 = 2$.
- Maximum iteration is set to $\text{iter}_{\max} = 1000$.
- Time for the optimization is $t = 100$ (s).

The default parameters of the function ga of MatLab, and $t = 100$ (s) of (12) are used for the GA algorithm. For the SQP method, the default parameters of the function $fmincon$ of MatLab are considered [19] and the initial conditions of the parameters are uniformly distributed in the search space.

3.3.2 Case 2

In practical requirements, the lower bounds of the controller parameters are $\text{LB}_\gamma = 0.1$ y $\text{LB}_\alpha = 0.01$, also, and the upper bounds $\text{UB}_\gamma = 9 \times 10^8$ and $\text{UB}_\alpha = 2$ which belong to the gains and orders of adaptive laws. For the FOMRAC controller, ω_l and ω_h in (3) are set to 0.001 and 1000 (rad/s), respectively, and the order of approximation in (3) is set to $N = 10$. For the PSO algorithm, the parameters used by [7] are defined as follows:

- The initial population cannot be chosen as in the technical literature, because this work is optimizing triple the number of parameters, and since the number of initial individuals is specific to each problem, 150 particles are defined.
- Inertia weight factor is set as (6) where $w_{\max} = 1.9$ and $w_{\min} = 0.4$.
- Acceleration constants $c_1 = 2$, $c_2 = 2$.
- Maximum iteration is set to $iter_{\max} = 1000$.
- Time for the optimization is $t = 10$ (s).

With the GA method, the default parameters of the function ga of MatLab, and $t = 10$ (s) in (13) are considered. For the SQP method, the default parameters of the function $fmincon$ of MatLab are used [19], and the initial conditions for the parameters are uniformly distributed in the search space.

As shown above, the values for the optimization parameters for each case study are not equal. This is because of the different time response of each generator model used.

4 Simulation results

This section presents the results obtained for the AVR controlled by the FOMRAC designed in Sect. 3. These results are compared with previous investigations. The fractional adaptive laws were implemented using the Ninteger Toolbox for Matlab Version 8.1.0.604(R2013a) [33].

4.1 Case study 1

The results obtained at this stage with OF_1 and the $Model_1$ in Fig. 2 will be compared to Aguila-Camacho et al. [1] and Zamani et al. [37].

4.1.1 Behavior of the MRAC

Several trials were performed for the optimization process to find the best set of controller parameters based on minimizing OF_1. The SQP and PSO algorithms obtained the best results. These are presented in Table 2, which will be compared with the results obtained by GA [1].

Figure 4 shows the step response of the controlled system, i.e., the voltage measured at the generator terminals. In this figure, two types of control are compared, which were taken from the literature. These are $IOPID_{GA}$ and $IOMRAC_{GA}$ versus $IOMRAC_{PSO,SQP}$, proposed in this case study. Also, the IOMRAC controllers have $O_s = 0$, while the $IOMRAC_{PSO}$
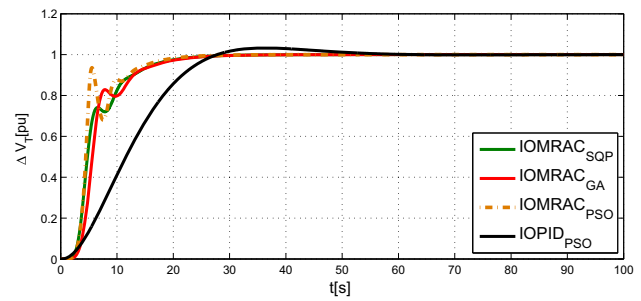

Fig. 4 Step responses of the AVR controlled by three IOMRACs, and IOPID

controller makes the system have a shorter settling time, t_s, than the $IOMRAC_{SQP}$ and $IOMRAC_{GA}$. The characteristics of the responses can be seen in Table 3.

Figure 5 corresponds to the evolution of field voltage of the synchronous machine. This exciter control action is responsible for maintaining the voltage at the generator terminals during a predefined operation. $MRAC_{PSO}$ has the lowest rise time t_r in relation to those presented earlier. The exciter control effort is the associated cost and is shown in Fig. 5.

Table 3 shows the details of the performance criteria associated with each method of optimization. Performance criteria (IAE, ITAE, ISE, ITSE) analyze behaviour of the error within time intervals $[0\ 100]s$.

In the case of fractional control (see Figs. 6 and 7), $FOMRAC_{PSO}$ shows significant improvements in terms of

Table 2 Gains and orders of adaptive laws, obtained by optimization algorithms Case Study 1

| | Differential orders α | | | | | | | | | | | |
	1	2	3	4	5	6	7	8	9	10	11	
IOMRAC												
GA	1	1	1	1	1	1	1	1	1	1	1	
SQP	1	1	1	1	1	1	1	1	1	1	1	
PSO	1	1	1	1	1	1	1	1	1	1	1	
FOMRAC												
GA	0.1508	0.4152	0.6000	0.1844	0.7627	0.2944	0.8110	0.9998	0.7024	0.1446	0.9885	
SQP	0.9304	0.0021	0.7522	0.9967	0.9973	0.0003	0.0051	0.0006	0.0001	0.0007	0.7470	
PSO	0.5641	0.0627	0.2419	0.0970	0.4194	0.6026	0.9979	0.8240	0.2006	0.0640	0.9999	
	Adaptive gains γ											OF_1
	1	2	3	4	5	6	7	8	9	10	11	
IOMRAC												
GA	1.814	10.179	11.449	9.969	4.522	3.844	1.254	5.130	0.391	1.823	20.399	127.35
SQP	4.671	6.147	3.455	7.709	7.417	4.857	5.816	2.784	4.872	4.784	37.426	127.12
PSO	3.936	13.920	31.494	33.367	50.000	24.575	33.367	32.226	9.398	16.733	7.564	123.83
FOMRAC												
GA	3.435	1.810	0.442	1.912	1.824	0.782	0.058	2.367	0.176	0.798	2.906	144.73
SQP	0.641	0.701	0.200	0.962	0.150	4.367	0.103	4.619	1.287	1.198	0.104	119.14
PSO	0.497	4.975	7.113	7.833	1.949	5.820	8.000	7.351	7.105	7.983	7.999	112.30

Table 3 Characteristics performance of step responses for Case Study 1

	Os (%)	Tr (s)	Ts (s)	Ess	OF1	IAE	ITAE	ISE	ITSE	J
IOMRAC										
GA	0	9.16	23.63	0.02	128.02	7.08	50.04	5.04	24.53	86.69
SQP	0	5.77	21.12	0.02	127.12	6.00	41.26	3.83	17.46	55.99
PSO	0	2.03	19.60	0.02	123.83	6.39	43.16	4.53	21.15	48.51
IOPID										
PSO	3.24	17.36	45.43	0.02	128.30	12.90	120.97	8.65	49.08	191.60
FOMRAC										
GA	0	13.84	34.55	0.02	144.77	8.70	80.90	5.03	17.33	111.96
SQP	0	4.48	16.51	0.02	119.14	8.42	53.00	6.82	25.00	72.69
PSO	0	4.87	10.65	0.02	112.30	7.82	34.39	6.64	23.57	72.42
FOPID										
PSO	0	26.70	53.57	0.02	143.11	11.87	172.58	5.38	31.53	222.07

OF_1 and t_s in relation to the integer order control or IOMRAC, which was shown above. At the same time, it is better than IOPID and FOPID presented by Aguila-Camacho et al. [1] and Zamani et al. [37], respectively. These are shown in Fig. 6 and their performance in Table 3.

Table 2 shows the values of the gains and the orders of adaptive laws for the MRAC controller. The lesser value, $OF_1 = 112.3$, is obtained using the PSO algorithm for the FOMRAC controller rather than IOMRAC, IOPID, and FOPID controllers. As can be seen from Table 3, the settling time t_s is shorter for the $FOMRAC_{PSO}$, since it improves

by 14.2 and 69.2% compared with the $IOMRAC_{GA}$ and the $FOMRAC_{GA}$ controllers, respectively, reported in [1]. In terms of the sum of the performance indices, the J of $FOMRAC_{PSO}$ is 34% better than J of $IOMRAC_{GA}$. Although a more demanding control signal is required as compared with the cases of FOPID and $FOMRAC_{GA}$, it has the same control effort as the $IOMRAC_{PSO}$. That is to say, the FOMRAC delivers a good balance between the transient response and the control signal behavior.

4.1.2 Robustness of the FOMRAC

The generator parameters may vary due to the wear of materials and changes in load. Therefore, the same robustness tests that were done in [1] will be performed here. Initially, the system is working in normal operation with the parameters set forth above; at $t = 100$ (s), parameter $K_1 = 1.59$ changes to $K_1 = 1$ due to changes in load conditions (Fig. 8).

According to [1], the result obtained by controller $FOMRAC_{GA}$ is better than FOPID in [37] regarding robustness tests. Figure 8 shows the best results obtained in this Case Study 1, which correspond to $FOMRAC_{PSO}$. These will be compared with the results obtained by $MRAC_{GA}$ [1],
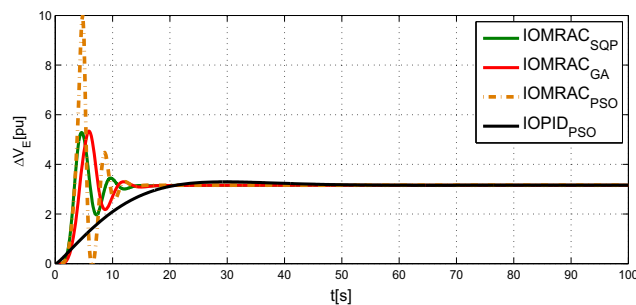

Fig. 5 Exciter control signals of the AVR controlled by the three IOMRAC's, and IOPID
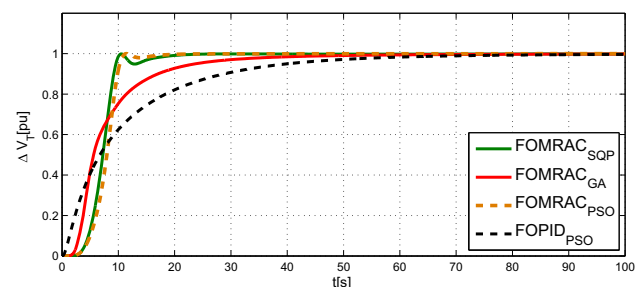

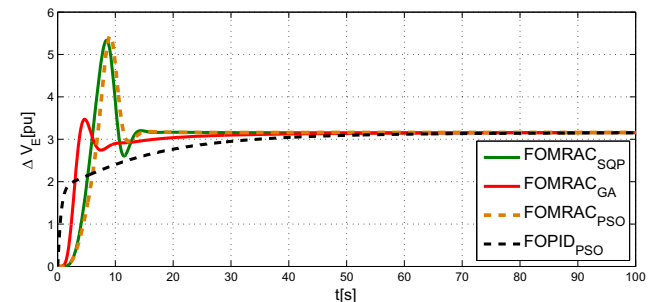**Fig. 6** Step responses of the AVR controlled by three FOMRACs, and FOPID

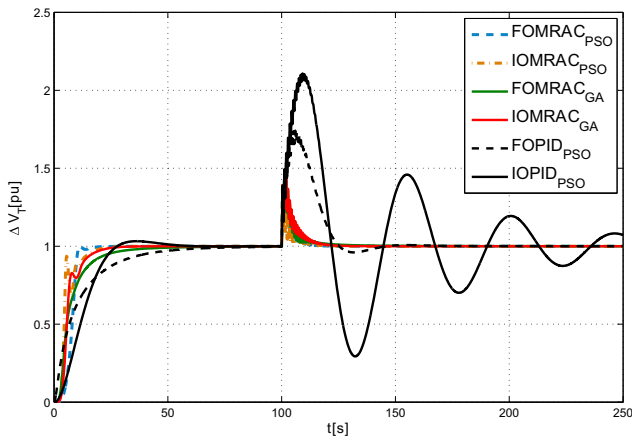**Fig. 7** Exciter control signals of the AVR controlled by the three FOMRACs, and FOPID

Fig. 8 Step responses of the AVR controlled of integer and fractional controllers, under a parameter variation in the generator at $t = 100$ (s)

Fig. 9 Field voltage of the AVR controlled by integer and fractional controllers, under a parameter variation in the generator at $t = 100$ (s)
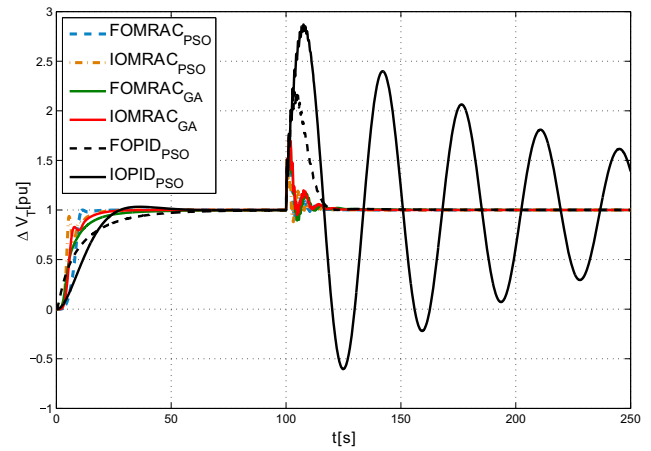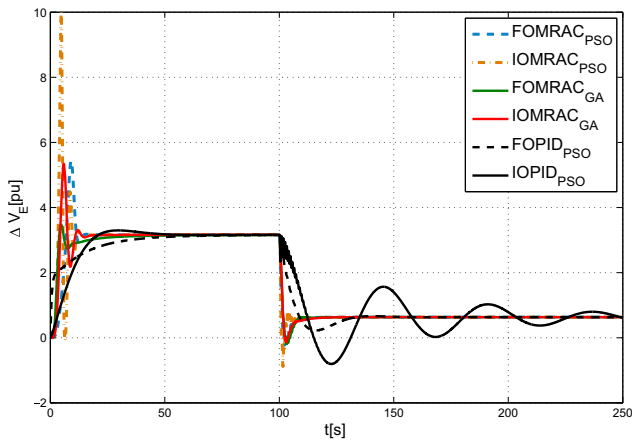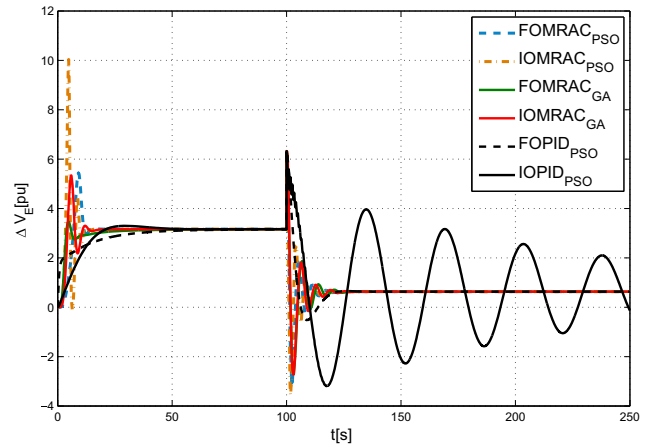

Fig. 10 Step responses of the AVR controlled of integer and fractional controllers, under variations in the parameters of the generator and the exciter transfer function at $t = 100$ (s)

Fig. 11 Exciter control signals of the AVR controlled of integer and fractional controllers, under variations in the parameters of the generator and the exciter transfer function at $t = 100$ (s)

and PID [37] of integer and fractional orders, and with the IOMRAC$_{PSO}$ controller of this work. Although the amplitude of the signal at the generator terminal voltage is the same in all four case MRAC controllers, the system controlled by FOMRAC$_{PSO}$ has less settling time than t_s of the system controlled by the FOMRAC$_{GA}$ controller. These are 15.6 and 26.8(s), respectively. Simply stated, the FOMRAC$_{PSO}$ controller stabilizes the system 41% faster than the FOMRAC$_{GA}$ controller. Furthermore, the amplified control action or the exciter system voltage is very similar to that of MRAC$_{GA}$ shown in Fig. 9.

In the second robustness test, another uncertainty in the exciter model was assumed, where the transfer function in (10) varies to $G_{E_1} = \frac{1}{0.5s+0.5}$ at $t = 100$ (s). For comparison, this test was taken from [1]. Fig. 10 shows the step response of the controlled system under variations occurring in the load and the excitation system.

It can be seen in Fig. 10 that the FOMRAC$_{PSO}$ controller improved 57% compared with the t_s obtained with the

FOMRAC$_{GA}$ controller. As far as control action is concerned, the exciter control action of the controller FOMRAC$_{PSO}$ does not have the associated cost shown in Fig. 11.

4.2 Case study 2

The results shown in this case study are obtained using the objective function OF$_2$ written as in (13), associated with Model$_2$. The simulation results will be compared with [7] and Mukherjee et al. [22] in which only an integer order PID controller is implemented for the AVR System. The gains for this control strategy were tuned by the PSO algorithm based on the objective function OF$_2$. The results obtained and reported in this paper show improvement over previous investigations, and will be developed in this section.

Referring to the special case of the AVR system analyzed by Chatterjee et al. [7], the parameters obtained by the opti-

Fig. 12 Block diagrams of
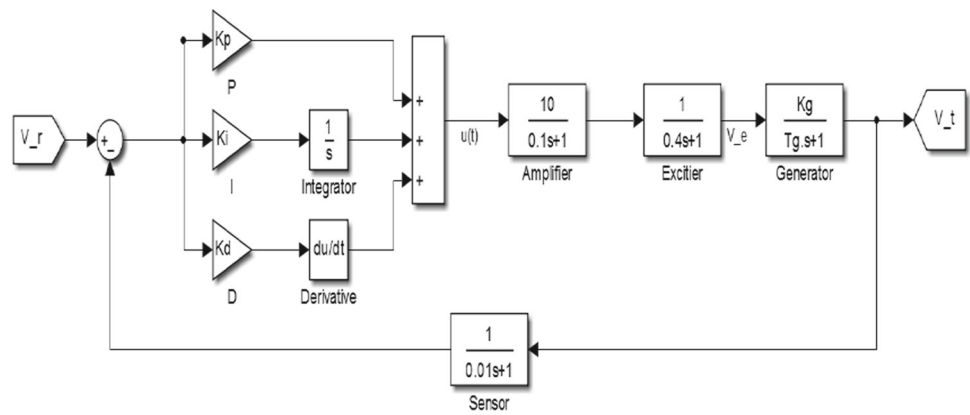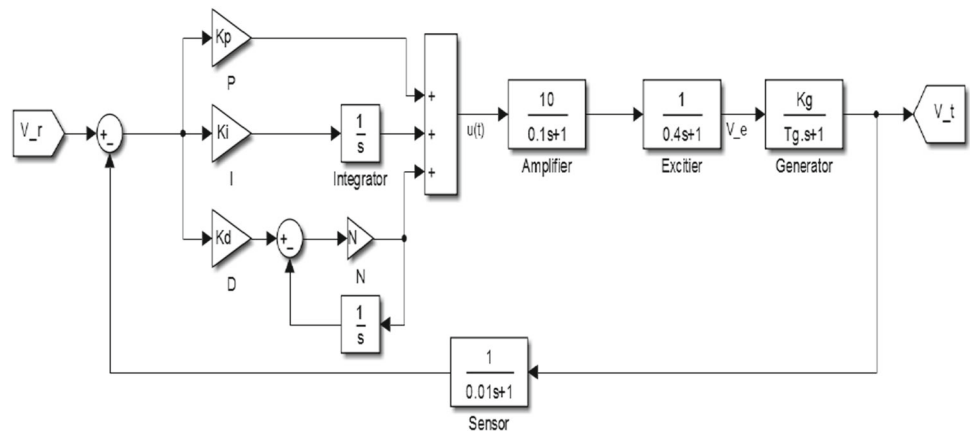continuous-time ideal PID
controller

Fig. 13 Block diagrams of
continuous-time filtered PID
controller

mization algorithm are $K_p = 0.6658$, $K_i = 0.4821$ and $K_d = 0.1963$. The closed-loop transfer function of the system controlled by PID is shown in that paper with the block diagram of Fig. 12. Unfortunately, we are unable to reproduce the figures shown by Chatterjee et al. [7]. It is due to the derivative action in [7] is filtered (see Eq. (16)), where $N = 100$ is the principal parameter for the filter. Therefore, the authors in [7] have not used an ideal PID controller like they highlight in their paper, but, a filtered PID controller shown in Fig. 13.

$$C(s) = K_p + \frac{K_i}{s} + K_d s \frac{N}{s + N} \qquad (16)$$

The ideal PID controller in the Laplace domain is $C(s) = K_p + \frac{K_i}{s} + K_d s$, which is an improper transfer function not supported by Simulink software because of the causality rule. Then MatLab adds a filter coefficient N to transfer function $C(s)$ in a continuous-time parallel PID controller as written in (16),

Figure 14a shows the responses of the control features of the PID$_{\text{FILTERED}}$ when $\Delta V_r(t) = 0.01$ are $t_s = 0.7$ (s), $O_s = 0.3\%$ and $\max - dv = 0.02$. Furthermore, $t_s = 3.9$ (s), $O_s = 11.4\%$ and $\max - dv = 0.02$ are the corresponding features of the PID$_{\text{IDEAL}}$. This aspect is important to emphasize since

comparisons are often made using the PID$_{\text{IDEAL}}$ (Pan et al. [26,27], Sahu et al. [29], Gozde et al. [13], dos Santos Coelho et al. [9] and the latest in Anwar et al. [3]).

Comparisons in this paper will be made with the results in [7], where the system is controlled by a filtered PID controller, as shown in Fig. 13 (indicated by red dash lines).

4.2.1 Behavior of the MRAC

In the SLM in (8), the damping phenomena are neglected. According to Kundur et al. [16], this is a small-signal model. Table 4 shows the gains and orders of the adaptive laws of the MRAC controllers obtained by the proposed optimization algorithms. Figure 15 shows the terminal voltage of the generator when the system is controlled by the IOMRAC controllers and an IOPID controller (Table 5).

The t_s of the best result obtained in this case study for the integer-order controllers corresponds to those of IOMRAC$_{\text{PSO}}$, which does not improve the results obtained by the researchers in [7] and shown in Fig. 15. However, comparisons can be made between the results obtained by optimization algorithms in terms of the objective function OF$_2$. The IOMRAC controller optimized by the PSO improves 55.1% over that obtained by the SQP algorithm and 96.4% to that of the GA algorithm.
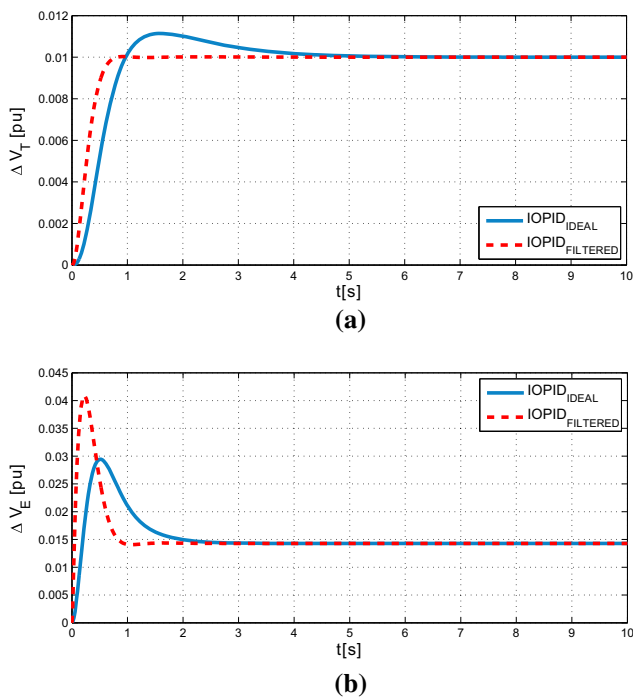
Fig. 14 **a** Step responses of the AVR controlled by the Ideal PID controller and the Filtered PID controller. **b** Control signals of the AVR controlled by the Ideal PID controller and the Filtered PID controller

The generator terminal voltage is controlled through the voltage on the field of the rotor ($\Delta V_E(t)$ shown in Fig. 16). The best result found in previous investigations corresponds to IOPID$_{PSO}$, where the cost associated is its exciter control signal, approximately 40% higher than IOMRAC$_{PSO}$. Practice shows that the fractional-order controller should provide better results considering the minimum performance criterion OF$_2$. This is due to the expansions of the search space, i.e., the order of $\alpha = 1$ changes to $\alpha \in [0, 2]$. Figure 17 presents the transient response of incremental change in terminal voltage for 1% step in reference voltage or $\Delta V_r = 0.01$ (pu).
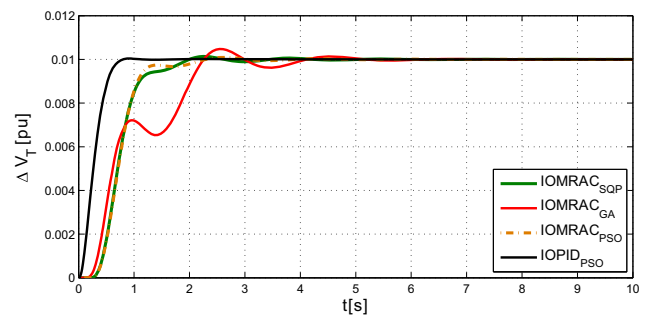

Fig. 15 Transient response of terminal voltage for a 0.01 (pu) step change in reference voltage, using integer-order controllers

Only the integer-order PID controller designed for AVR appears in previous investigations. To emphasize the advantages of fractional-order controllers, a FOPID controller was also designed using the same method depicted in Fig. 14a. The same evaluation function as in [32,38] was used, in which the parameters obtained by the PSO algorithm are the gains $K_p = 1.5338$ $K_i = 0.6523$, $K_d = 0.9722$, $\alpha = 0.9722$ is the fractional-order integral action, and $\beta = 1.2090$, is the fractional-order derivative action.

Figures 17 and 18 show three FOMRAC controllers optimized by SQP, GA and PSO, and a FOPID$_{PSO}$ controller. Although the FOPID$_{PSO}$ performance is better than FOMRAC in terms of t_s, it has a high cost for the voltage in the excitation system as shown in Fig. 18. Furthermore, the performance of FOPID$_{PSO}$ proposed here is 85% lower than the IOPID$_{PSO}$ in terms of OF$_2$. The MRAC has higher robust stability than the IOPID, as is observed in the following simulations.

4.2.2 Robustness test

Robustness tests are performed to analyze the controlled system behavior under parametric variations. The PSO optimization algorithm associated with the FOPID controller obtained the best results for the evaluation function OF$_2$. The

Table 4 Gains and orders of adaptive laws, obtained by optimization algorithms Case Study 2

	ALPHA					GAMMA					OF2
	1	2	3	4	5	1	2	3	4	5	
IOMRAC											
GA	1	1	1	1	1	150,075,519.96	471,452,555.67	193,523,152.02	634,051,780.56	882047330.78	2.25E+09
SQP	1	1	1	1	1	136,455,975.70	639,308,187.82	690,803,328.56	872,560,567.79	876822473.11	1.82E+08
PSO	1	1	1	1	1	125,930,508.02	373,843,038.68	462,069,378.71	739,689,316.27	899918348.78	8.18E+07
FOMRAC											
GA	0.87	1.22	0.04	0.02	1.11	353,004,378.43	581,681,745.29	492,494,022.36	825,474,306.66	701,250,529.76	2.37E+08
SQP	0.36	0.42	0.31	0.42	0.80	186,968,063.72	271,121,697.62	423,831,013.55	207,439,344.25	759,877,913.31	1.16E+09
PSO	1.10	0.37	0.18	0.96	1.38	8,333,153.52	752,265,696.35	527,845,557.08	619,790,700.47	616,252,640.16	22.27

Table 5 Performance criteria Case Study 2

	FOMRAC			FOPID	IOMRAC			IOPID
	SQP	GA	PSO	PSO	SQP	GA	PSO	VURPSO
tr (s)	0.89	0.93	0.84	0.19	0.66	1.68	0.62	0.43
ts (s)	3.54	1.38	3.26	0.58	1.83	3.84	2.01	0.68
Os (%)	3.41	1.54	0	0	1.35	4.74	0.90	0.34
max − dv	0.0133	0.0166	0.0130	0.0533	0.0168	0.0194	0.0116	0.0036
J	0.0165	0.0128	0.0205	0.0063	0.0119	0.0162	0.0166	0.0250
OF2	1.16E+09	2.37E+08	22.27	0.68	1.82E+08	2.25E+09	8.18E+07	1.18E+07
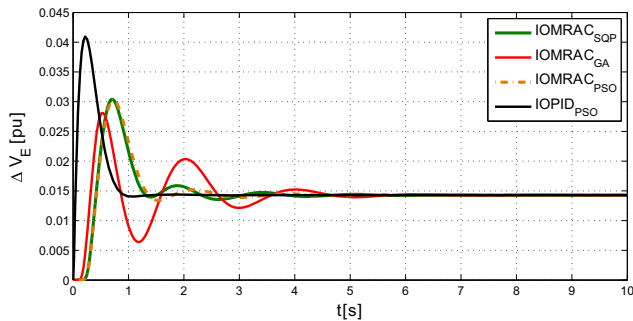
Fig. 16 Exciter control signals of the AVR controlled by the IOMRAC$_{SQP}$, IOMRAC$_{GA}$, IOMRAC$_{PSO}$ and PID controllers
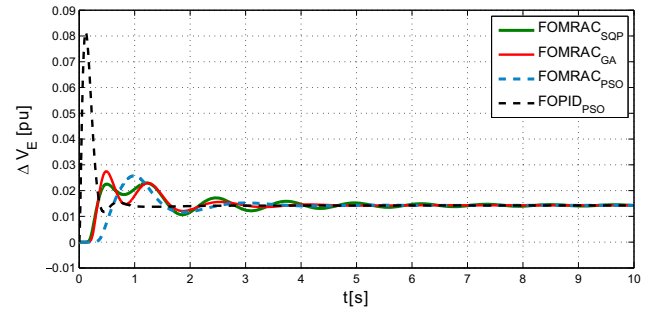
Fig. 18 Exciter control signals of the AVR controlled by the FOMRAC$_{SQP}$, FOMRAC$_{GA}$, FOMRAC$_{PSO}$ and FOPID controllers
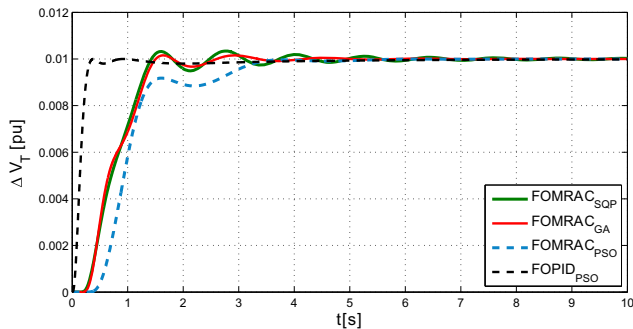

Fig. 17 Transient response of incremental change in terminal voltage for a 0.01 (pu) step change in reference voltage, using fractional-order controllers
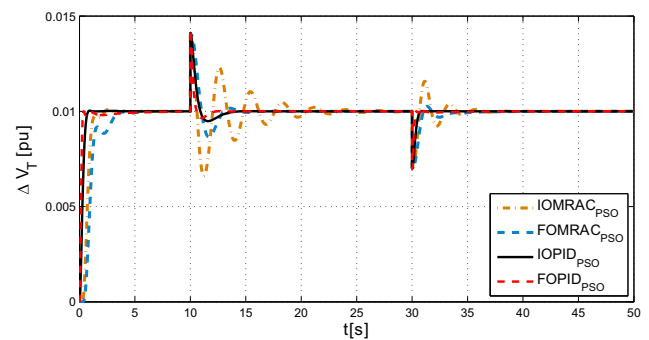

Fig. 19 Step responses of the AVR controlled by the MRAC$_{PSO}$ and PID$_{PSO}$ of integer and fractional orders, under variations in the parameters of the generator at different times

robustness tests will show the real benefits of the controllers IOMRAC$_{PSO}$ and FOMRAC$_{PSO}$.

Tuned parameters for the PID controller are constant over time, but the parameters obtained by the MRAC vary with the tracking error. This is the main feature that stands out for the controllers presented in this paper.

The first robustness test conducted in this Case Study 2 corresponds to variations in the parameters of the generator. At $t = 10$ (s), $K_G = 0.7$ and $\tau_G = 1$ change to $K_G = 0.87$ and $\tau_G = 2.5$, respectively. Later, at $t = 30$ (s), the parameters retake the parameters of the initial operating conditions. These are depicted in Fig. 19 to examine the robustness of the fractional controllers numerically. It can be seen that the

t_s of the FOPID$_{PSO}$ controller is 11.1% less rather than the t_s of the PID$_{PSO}$ controller. Furthermore, the evaluation function OF$_2$ of the FOMRAC$_{PSO}$ controller is 4.2% less than the OF$_2$ of the PID$_{PSO}$ (Chatterjee et al. [7]).

Based on the additional performance index (J), it is shown that the best results in terms of error dynamics are those with the FOPID$_{PSO}$ controller. It improves performance by 28% compared to the IOPID$_{PSO}$ controller reported in [7]. We can see that the adaptive strategies controls depicted in Fig. 20 are tripled compared with the exciter action control $\Delta V_E(t)$. However, this value is within the operating range of the excitation system.
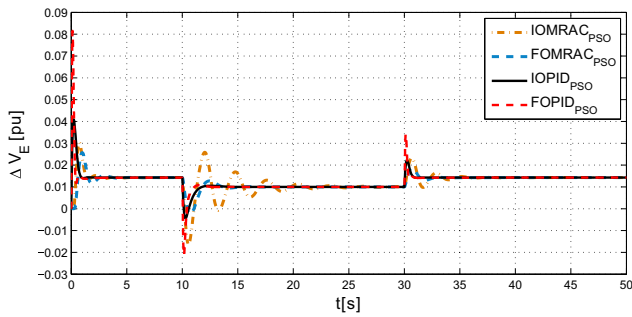
Fig. 20 Exciter control signals of the AVR controlled by the MRAC$_{PSO}$ and PID$_{PSO}$ of integer and fractional orders, under variations in the parameters of the generator at different times
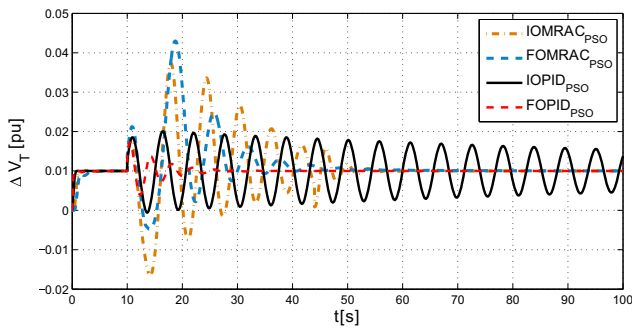

Fig. 21 Step responses of the AVR controlled by the MRAC$_{PSO}$ and PID$_{PSO}$ of integer and fractional orders, under variations in the parameters of the generator and the exciter transfer function

In the second robustness test, another uncertainty of the exciter model was assumed, in which the transfer function varies from $G_E(s) = \frac{1}{0.5s+1}$ to $G_{E1} = \frac{2}{5s+1}$ at $t = 10$ (s). The behavior is shown in Fig. 21.

The analyses of the different control schemes show the advantages and disadvantages of fractional order control. The IOPID$_{PSO}$ controller fails to stabilize the system within the defined time interval, compared to FOPID$_{PSO}$, which stabilizes the system in $t_s = 18$ (s). Then, the fractional-order controller demonstrates its robustness under parametric variations.

In this context, the MRAC$_{PSO}$ controller proposed in this paper satisfies the aim of the control in 43.9 (s) after the parameter variations. However, the FOMRAC$_{PSO}$ controller offers an 8.2% improvement in settling time compared with the IOMRAC$_{PSO}$ controller. The performance criteria arithmetic sum offers a valuable tool for evaluating controlled systems. In this case, the J of the FOMRAC$_{PSO}$ controller are 37.9% less than the J of the IOMRAC$_{PSO}$ controller.

Finally, the results obtained by the FOPID$_{PSO}$ controller are more efficient than those of the IOPID$_{PSO}$. The magnitude of the exciter control action is depicted in Fig. 22. However, the FOMRAC$_{PSO}$ controller is still a good alternative for the AVR systems.
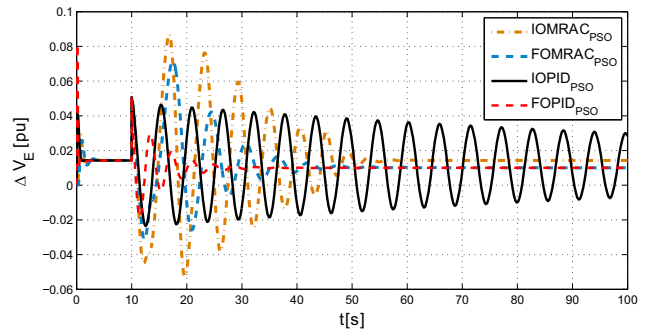
Fig. 22 Exciter control signals of the AVR controlled by the MRAC$_{PSO}$ and PID$_{PSO}$ of integer and fractional orders, under variations in the parameters of the generator and the exciter transfer function at different times
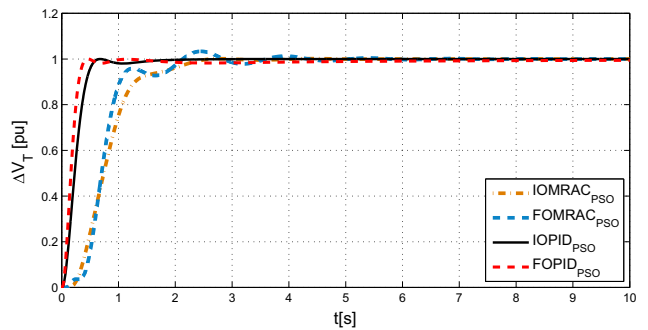

Fig. 23 Terminal voltage signals of the AVR controlled by the MRACs, and PIDs
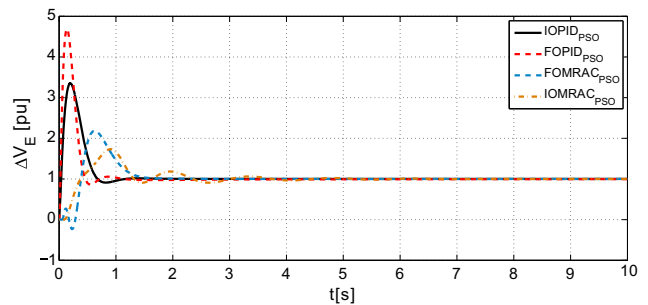

Fig. 24 Exciter control signals of the AVR controlled by the MRACs, and PIDs

4.3 Case study 3

This case is used to confirm the results obtained in the two previous cases. It will test the advantages of the fractional-order controllers in relation to the integer order ones. The results shown in this case study are performed using the objective function OF$_2$ written as (13), associated with Model$_2$. The difference with Case Study 2 is that the change of the reference voltage is chosen as $\Delta V_r = 1$ (pu) and the gain of the generator $K_G = 1$. As there is no standard cost function, we use OF$_2$ in the simulations test. To start with, the parameters of the integer- and fractional-order PID con-

Table 6 Gains and orders of adaptive laws, obtained by optimization algorithms Case Study 3

| | ALPHA | | | | | GAMMA | | | | | OF2 |
	1	2	3	4	5	1	2	3	4	5	
IOMRAC	1	1	1	1	1	8,228,347.7	500,000,000.0	303,459,790.9	196,829,082.1	317,820,160.0	2.66E+08
FOMRAC	0.86	1.367	1.53	1.339	1.218	300,000,000.7	54,938,608. 0	600,000,000. 3	600,000,000. 3	600,000,000.3	4.63E+07

troller are tuned, and then, the MRAC controllers are chosen using the PSO optimization technique. Finally, performance indices that assess the advantages and disadvantages of each type of control are assumed.

Before proceeding with the numerical analysis of these results, it is necessary to introduce the parameters obtained for the PID controller. These are $K_p = 0.54455$, $K_i = 0.36898$, $K_d = 0.17382$ for the IOPID$_{PSO}$, and $\alpha = 0.8448$, $\beta = 1.1123$, $K_p = 0.7697$, $K_i = 0.5171$, $K_d = 0.2302$ for the FOPID$_{PSO}$.

4.3.1 Behaviour of the MRAC

The parameters obtained for the integer- and fractional-order MRAC$_{PSO}$ controllers are shown in Table 6. Note that the PSO optimization algorithm is used because it shows significant advantages compared with the other optimization techniques for the AVR systems. The results are shown in Fig. 23.

According to Table 7, the settling time t_s of the FOMRAC$_{PSO}$, is 8.5% less than t_s of the IOMRAC$_{PSO}$. On the other hand, the t_s of the FOPID$_{PSO}$ is 31.1% less than t_s of the IOPID$_{PSO}$.

The integer- and fractional-order PID$_{PSO}$ controllers use triple the exciting voltage compared with the adaptive strategies control MRAC$_{PSO}$. The exciter voltage control $\Delta V_E(t)$ is shown in Fig. 24. The magnitude of the exciter control signal exceeds the operating ranges, which is due to ΔV_r changes of 100% of the rated voltage of the AVR system.

4.3.2 Robustness test

At this stage, the benefits of each strategy of the fractional-order controller are emphasized. As in the previous case

Table 7 Performance criteria, obtained by the controllers with optimized parameters Case Study 3

	IOMRAC	FOMRAC	IOPID	FOPID
tr (s)	0.931	0.505	0.346	0.236
ts (s)	2.221	2.033	0.547	0.377
Os (%)	0.151	0.680	0	0
max − dv	1.103	2.093	2.975	4.314
J	2.071	1.811	0.513	0.873
OF2	2.27E+06	4.63E+07	0.30	0.14

studies, changes can occur in the system parameters for different reasons. The parameters change from $K_G = 1$, $\tau_G = 1$ to 0.87 and 2.5, respectively. Another uncertainty in the exciter model was assumed in the robustness test, where the transfer function varies from $G_E(s) = \frac{1}{0.4s+1}$ to $G_E(s) = \frac{2}{6s+1}$ at $t = 10$ (s). These changes represent the state of maximum stress of the AVR system.

As can be seen in Fig. 25, the time interval starts at $t = 10$ (s) and goes to $t = 100$ (s), to emphasize the advantage of the FOPID$_{PSO}$ controller in comparison with the IOPID$_{PSO}$ controller. The FOPID$_{PSO}$ controller does not have an associated cost, since ΔV_E is like the ΔV_E of the IOPID$_{PSO}$ controller.

For the MRAC controllers, the advantages of the FOMRAC$_{PSO}$ controller in relation to the controller IOMRAC$_{PSO}$ are noted one more time. The OF$_2$ of the
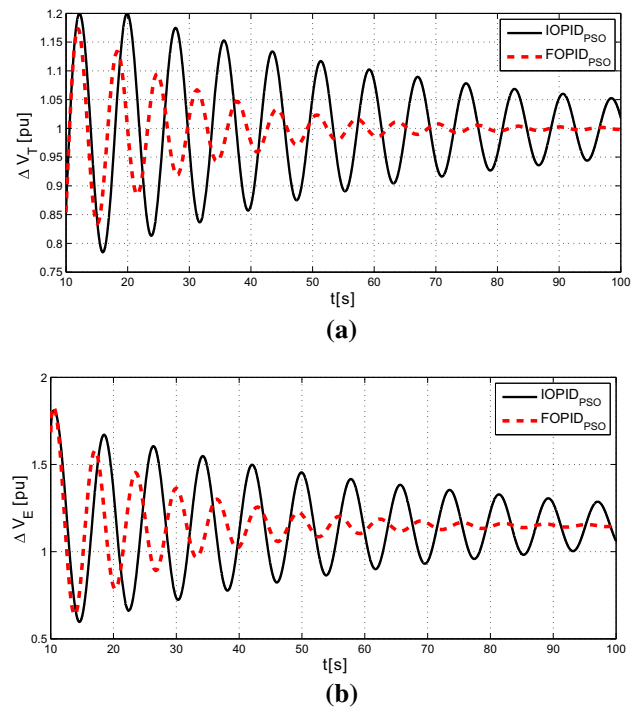

Fig. 25 a Step responses of the AVR controlled by the integer- and fractional-order PID$_{PSO}$ controllers, under variations in the parameters of the generator and the exciter transfer function at $t = 10$ (s). **b** Exciter control signals of the AVR controlled by the integer- and fractional-order PID$_{PSO}$ controllers under variations in the parameters of the generator and the exciter transfer function at $t = 10$ (s)
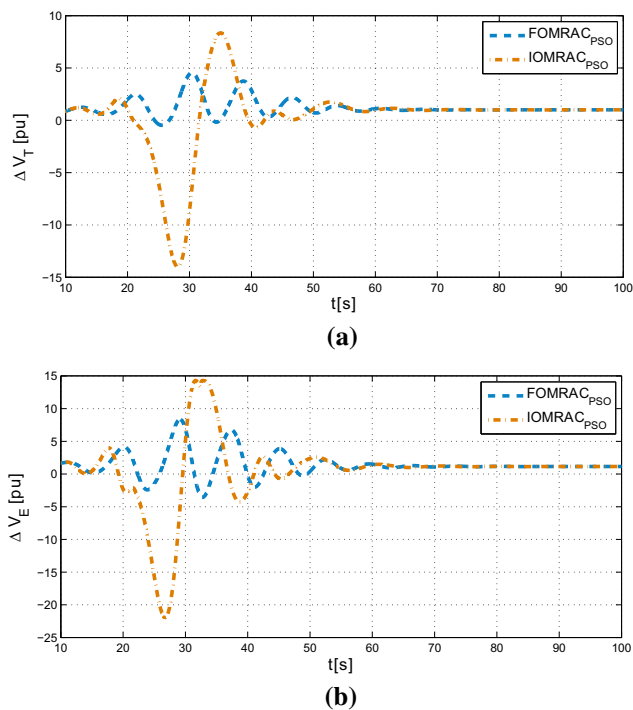
(a)

(b)

Fig. 26 **a** Step responses of the AVR controlled by the integer and fractional order MRAC$_{PSO}$ controllers, under variations in the parameters of the generator and the exciter transfer function at $t = 10$ (s). **b** Exciter control signals of the AVR controlled by the integer- and fractional-order MRAC$_{PSO}$ controllers under variations in the parameters of the generator and the exciter transfer function at $t = 10$ (s)

FOMRAC$_{PSO}$ is 76.6% less than the OF$_2$ of the IOMRAC$_{PSO}$, due to the value of O_s, and shown in Fig. 26a. Furthermore, the voltage of the excitation system shows that despite the improvement, there is not an associated cost, (it is even smaller as is shown in Fig. 26b). Another important feature is the t_s, since the FOMRAC$_{PSO}$ controller exhibits a shorter settling time of about 42.3 (s) compared to the 45.3 (s) of the IOMRAC$_{PSO}$ controller.

Defining $t = 100$ (s) and the error like $e_c(t) = r(t) - y_p(t)$, the IOPID$_{PSO}$ controller exhibits lesser J of about 340.1 compared to 76.9 for the FOPID$_{PSO}$ controller, 90.7% improvement . On the other hand, the controller FOMRAC$_{PSO}$ exhibits lower J of about 3670.9 compared to 36867.7 for the IOMRAC$_{PSO}$ controller, a 90% improvement.

5 Conclusions

This paper presents the application of FOMRAC and FOPID to an AVR system. The gains and fractional orders are selected through optimization algorithms. Different optimization procedures in regard to the minimization of two evaluation functions associated with two models used for the AVR system are considered.

In Case Study 1, the FOMRAC$_{PSO}$ controller improves the t_s by 47.2% over that reported in [1]. Furthermore, simulation studies show an improvement in characteristics of the response of the controlled system and in robustness with respect to model uncertainties when using the FOMRAC$_{PSO}$ controller. The FOMRAC$_{PSO}$ proposed in this paper improves the fitness function OF$_1$ by 58.8% compared with that reported for FOPID$_{PSO}$ by Zamani et al. [37].

In Case Study 2, the simplification of the MRAC controller is done since the simplified linear model of an AVR system is used. The evaluation of each control structure is performed, finding an improvement in characteristics of the response of the controlled system and in robustness with respect to model uncertainties when using the fractional-order controller, since there is an improvement of 97.9% with the FOPID$_{PSO}$ compared to OF$_2$ of the IOPID$_{PSO}$ reported in [7]. Moreover, the controller FOMMRAC$_{PSO}$ improves performance by 37.9% compared to IOMRAC$_{PSO}$ based on the sum performance indices (J) used to evaluate the behavior of the controllers.

To verify the advantages discussed, Case Study 3 is performed. The advantages of the fractional-order controllers in relation to the integer-order controllers is confirmed. This is based on the sum performance indices, when there are uncertainties in the plant.

For all optimization procedures, generalization to fractional-order controllers (FOPID and FOMRAC) present better results in terms of settling times. Also, OF$_1$ and OF$_2$ are improved at the minimum for each performance criterion evaluated in this work. Furthermore, it can be concluded from the above simulations that fractional order control is robust against variations in the internal parameters of the plant model. Many performance measures which assess the advantages and disadvantages of fractional control, were analyzed in this work, demonstrating the evident benefits of its application.

References

1. Aguila-Camacho N, Duarte-Mermoud MA (2013) Fractional adaptive control for an automatic voltage regulator. ISA Trans 52(6):807–15
2. Andersson G, Bel CA, Cañizares C (2009) Frequency and Voltage Control. In: Gómez-Expósito A, Conejo A (eds) Electric energy systems: analysis and operation, Chap. 9. CRC Press, Burgos Province, pp 355–399

3. Anwar MN, Pan S (2014) A frequency domain design of PID controller for an AVR system. J Zhejiang Univ Sci C 15(4):293–299
4. Betts JT, Frank PD (1994) A sparse nonlinear optimization algorithm. J Optim Theory Appl 82(3):519–541
5. Boggs PT (1996) Sequential Quadratic Programming. Ph.D. thesis, Departments of Mathematics and Operations Research-University of North Carolina
6. Chapman SJ (2006) Máquinas Eléctricas 2006, tercera, ed edn. British Aerospace Australia, Australia
7. Chatterjee A, Mukherjee V, Ghoshal S (2009) Velocity relaxed and craziness-based swarm optimized intelligent PID and PSS controlled AVR system. Int J Electr Power Energy Syst 31(7–8):323–333
8. Conceicao I (2008) Quantum Gaussian particle swarm optimization approach for PID controller design in AVR system. In: Proceedings International Conference on Systems, Man and Cybernetics vol 2, pp 3708–3713
9. dos Santos Coelho L (2009) Tuning of PID controller for an automatic regulator voltage system using chaotic optimization approach. Chaos Solitons Fractals 39(4):1504–1514
10. Eldersveld SK (1991) Large-scale sequential quadratic programming algorithms. Ph.D. thesis, Department of Operations Research-Stanford University, Stanford
11. Gaing ZL (2004) A particle swarm optimization approach for optimum design of PID controller in AVR system. IEEE Trans Energy Convers 19(2):384–391
12. Gallegos J, Duarte-Mermoud MA (2016) Mixed order robust adaptive control for general linear time invariant systems. J Frankl Inst (2016) (**submitted to**)
13. Gozde H, Taplamacioglu M (2011) Comparative performance analysis of artificial bee colony algorithm for automatic voltage regulator (AVR) system. J Frankl Inst 348(8):1927–1946
14. Kennedy J, Eberhart R (1995) Particle swarm optimization. IEEE 95:1942–1948
15. Kilbas AA, Srivastava HM, Trujillo JJ (2006) Theory and applications of fractional differential equations. Elsevier B.V, San Diego
16. Kundur P (1994) Power system stability and control. Palo Alto, California
17. Ladaci S, Charef A (2009) Robust fractional adaptive control based on the strictly positive realness condition. Int J Appl Math Comput Sci 19(1):69–76
18. Ladaci S, Charef A, Loiseau JJ (2006) On fractional adaptive control. Nonlinear Dyn 43(4):365–378
19. Math Work: fmincon SQP Algorithm (2014). https://www.mathworks.com/
20. MathWork: Genetic Algorithm (2014). https://www.mathworks.com/
21. Mukherjee V, Ghoshal S (2007) Comparison of intelligent fuzzy based AGC coordinated PID controlled and PSS controlled AVR system. Int J Electr Power Energy Syst 29(9):679–689
22. Mukherjee V, Ghoshal S (2007) Intelligent particle swarm optimized fuzzy PID controller for AVR system. Electric Power Syst Res 77(12):1689–1698
23. Narendra KS, Annaswamy AM (2005) Stable adaptive systems. Dover Publications Inc., Mineola
24. Ordóñez-Hurtado RH (2012) Aplicación de la técnica PSO a la determinación de funciones de Lyaunov cuadráticas comunes y a sistemas adaptables basados en modelos de error. Ph.D. thesis, Departamento de Ingeniería Eléctrica, Universidad De Chile
25. Oustaloup A (1991) La commande CRONE: commande robuste d'ordre non entier. Hermes, USA
26. Pan I, Das S (2012) Chaotic multi-objective optimization based design of fractional order $PI\lambda D\mu$ controller in AVR system. Int J Electr Power Energy Syst 43(1):393–407
27. Pan I, Das S (2013) Frequency domain design of fractional order PID controller for AVR system using chaotic multi-objective optimization. Int J Electr Power Energy Syst 51:106–118
28. Panda S, Sahu B, Mohanty P (2012) Design and performance analysis of PID controller for an automatic voltage regulator system using simplified particle swarm optimization. J Frankl Inst 349(8):2609–2625
29. Sahu BK, Mohanty PK, Panda S, Kar SK, Mishra N (2012) Design and comparative performance analysis of PID controlled automatic voltage regulator tuned by many optimizing liaisons. In: Proceedings of the 2012 International Conference on Advances in Power Conversion and Energy Technologies (APCET), pp 1–6. IEEE
30. Sfaihi B, Boubaker O (2004) Full order observer design for linear systems with unknown inputs. In: IEEE International Conference on Industrial Technology. IEEE ICIT'04, vol 3, no 5, pp 1233–1238
31. Shi Y, Eberhart R (1999) Empirical study of particle swarm optimization. In: Proceedings of the 1999 Congress on Evolutionary Computation-CEC99 (Cat. No. 99TH8406), pp 1945–1950
32. Tang Y, Cui M, Hua C, Li L, Yang Y (2012) Optimum design of fractional order $PI\lambda D\mu$ controller for AVR system using chaotic ant swarm. Expert Syst Appl 39(8):6887–6896
33. Valério D (2005) Ninteger v. 2.3 Fractional control toolbox for MatLab. https://www.mathworks.com/
34. Valério D, da Costa JS (2004) Ninteger: a non-integer control toolbox for MatLab. In: Proceedings of the First IFAC Workshop on Fractional Differentiation and Applications. Bordeaux, France, pp 208–213
35. Vinagre BM, Petras I, Podlubny I, Chen YQ (2002) Using fractional order adjustment rules and fractional order reference models in model reference adaptive control. Nonlinear Dyn 29(1–4):269–279
36. Wildi T (2007) Máquinas Eléctricas y Sistemas De Potencia. Pearson ed edn, México
37. Zamani M, Karimi-Ghartemani M, Sadati N, Parniani M (2009) Design of a fractional order PID controller for an AVR using particle swarm optimization. Control Eng Pract 17(12):1380–1387
38. Zhu H, Li L, Zhao Y, Guo Y, Yang Y (2009) CAS algorithm-based optimum design of PID controller in AVR system. Chaos Solitons Fractals 42(2):792–800